WRF Mesoscale Pre-Run for the Wind Atlas of Mexico

Hahmann, Andrea N.; Pena Diaz, Alfredo; Hansen, Jens Carsten

Publication date:
2016

Document Version
Publisher's PDF, also known as Version of record

WRF Mesoscale Pre-Run for the Wind Atlas of Mexico

Department of Wind Energy
E Report 2016

Andrea N. Hahmann, Alfredo Peña and Jens Carsten Hansen

DTU Wind Energy E-0126

June 2016

DTU Wind Energy Report E-0126

WRF Mesoscale Pre-Run for the Wind Atlas of Mexico

Andrea N. Hahmann, Alfredo Peña and Jens Carsten Hansen

DTU Wind Energy
Department of Wind Energy

DTU Wind Energy, Risø Campus,
Technical University of Denmark, Roskilde, Denmark

June 2016

Author: Andrea N. Hahmann, Alfredo Peña and Jens Carsten Hansen
Title: WRF Mesoscale Pre-Run for the Wind Atlas of Mexico
Department: DTU Wind Energy

DTU Wind Energy Report E-0126
June 28, 2016

Abstract (max. 2000 char)

This report documents the work performed by DTU Wind Energy for the project "Atlas Eólico Mexicano" or the Wind Atlas of Mexico. This document reports on the methods used in "Pre-run" of the wind-mapping project for Mexico. The interim mesoscale modeling results were calculated from the output of simulations using the Weather, Research and Forecasting (WRF) model. We document the method used to run the mesoscale simulations and to generalize the WRF model wind climatologies. A separate section covers the preliminary validation of the WRF simulations against tall mast observations.

ISSN:
ISBN:
978-87-93278-88-2

Contract no:
N/A

Project no:
N/A

Sponsorship:
Bilateral agreement on Climate Change Mitigation and Energy Programme

Pages: 25
Tables: 5
Figures: 15
References: 10

Technical University of Denmark
Frederiksborgvej 399
4000 Roskilde
Denmark
Tel. +4546775024
ahah@dtu.dk
www.vindenergi.dk

Contents

1 Introduction

Numerical wind atlas methodologies have been devised to solve the issue of insufficient wind measurements. The method developed at DTU Wind Energy uses the Weather Research and Forecasting (WRF) model in a dynamical downscaling mode to produce mesoscale analysis. The method has recently been documented in Hahmann et al. (2015) and verified against tall masts in the North and Baltic Sea. The same method was used and documented in the recent Wind Atlas for South Africa (Hahmann et al., 2014).

This document reports on the methods used in Phase 1 of the "Wind Atlas for Mexico" project. The interim mesoscale modeling results were calculated from the output of simulations using the Weather, Research and Forecasting (WRF) model. We document the method used to run the mesoscale simulations and to generalize the WRF model wind climatologies. We also describe the special WRF model settings used in previous numerical wind atlas projects and set here to cover the landscape and geography of Mexico. However, the WRF simulations themselves were not optimized to the wind climate of Mexico.

The results of the simulations presented here are from what we call a "WRF Pre-run" simulations. The preliminary verification is crude because many of the meteorological masts used for validation have not specifically designed with the objective of verifying a numerical wind atlas. The results of the simulations in this report are only intended for aiding in the site selection for new wind masts to verify a future numerical wind atlas. Also the results provide useful information for identifying areas were more attention should be paid to in the sensitivity studies for the final run of the wind atlas. The results are preliminary and not intended for further wind energy development.

2 WRF setup

The simulations described here use the Advanced Research WRF (ARW-WRF) version 3.5.1 model released on 23 September 2013. The WRF modeling system is in the public domain and is freely available for community use. It is designed to be a flexible, state-of-the-art atmospheric simulation system that is portable and efficient on available parallel computing platforms. The WRF model is used worldwide for a variety of applications, from real-time weather forecasting, regional climate modeling, to simulating small-scale thunderstorms.

We carried out preliminary simulations using the WRF model for the Mexican territory. The details of the WRF setup are shown in Table 1 (the actual model namelist is included as an attachment at the end of this document). The simulation covers the period from October 2005 to September 2015 and was run in a series of 11-day long overlapping simulations, with the output from the first day being discarded. This method is based on the assumptions described in Hahmann et al. (2010). The simulation used grid nudging that continuously relaxes the model solution towards the gridded reanalysis (every 6 h) but this was done only on the outer domain and above the boundary layer (level 10, located $\approx$1000 m AGL) to allow for the mesoscale processes near the surface to develop freely. The domain configuration is shown in Fig. 1. The grid has been rotated to best cover the Mexican land area. In the vertical, the model was configured with 41 levels with model top at 50 hPa. The lowest 10 levels are within 1000 m of the surface and the first level is located at approximately 14 m AGL.

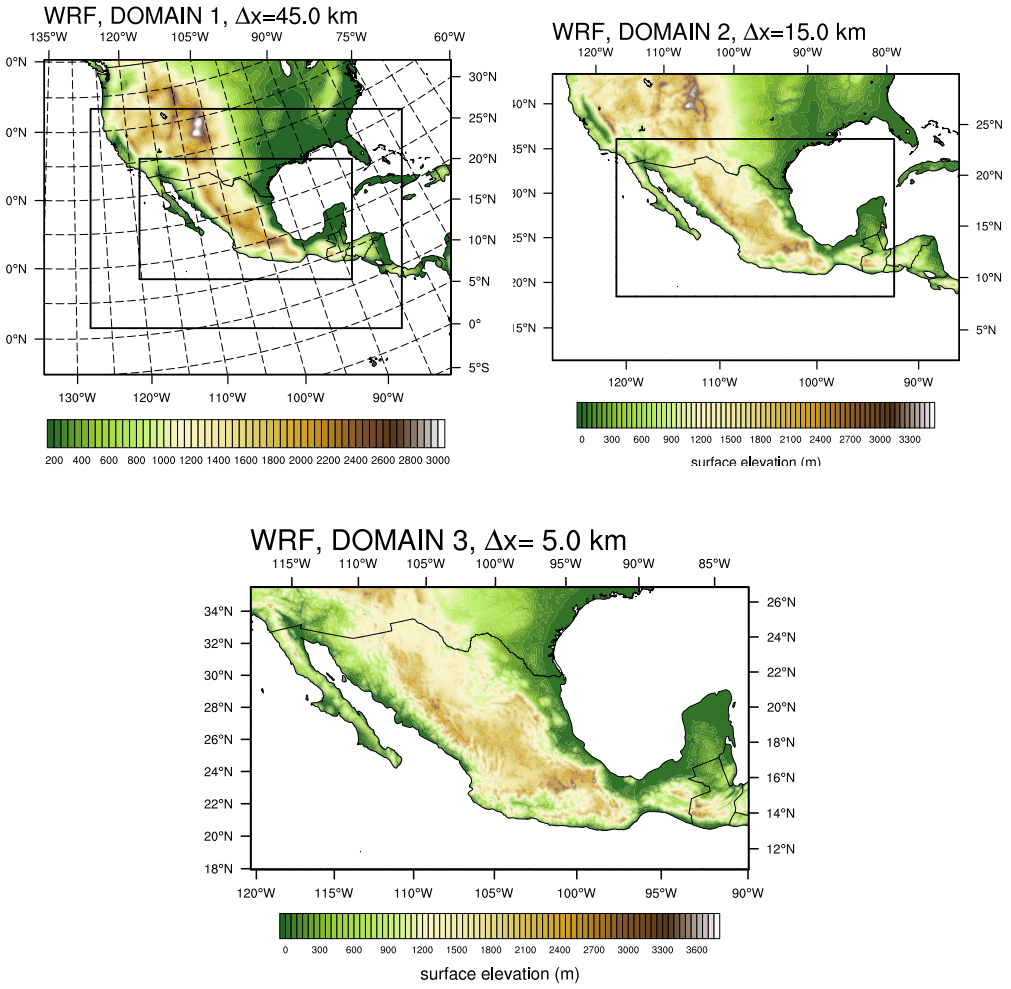

Figure 1: WRF model domain configurations and terrain elevation (m). Top left: 45 km $\times$ 45 km domain (D1), Top right: 15 km $\times$ 15 km (D2) and Bottom: 5 km $\times$ 5 km (D3). The inner lines show the position of D2 and D3 in D1 and D2, respectively.

Model setup:
WRF (ARW) Version 3.5.1.
Mother domain (D1; 147 $\times$ 114 grid points) with 45 km grid spacing; 2 nested domains: D2 (336 $\times$ 237 grid points) using 15 km and D3 (687 $\times$ 390 grid points) 5 km horizontal grid spacing on a lambert projection (see Fig. 1).
41 vertical levels with model top at 50 hPa; 10 of these levels are placed within 1000 m of the surface; The first 6 levels are located approximately at: 14, 43, 72, 100, 129 and 190 m.
MODIS (2001–2010) land-cover classification of the International Geosphere-Biosphere Programme.
Changes to lakes for better representation of inland water bodies.
Simulation setup:
Initial, boundary conditions, and fields for grid nudging come from the European Centre for Medium Range Forecast (ECMWF) ERA-Interim Reanalysis (Dee et al., 2011) at 0.75° $\times$ 0.75° resolution.
Runs are started (cold start) at 00:00 UTC every 10 days and are integrated for 11 days, the first 24 hours of each simulation are disregarded.
Sea surface temperature (SST) and sea-ice fractions come from the dataset produced at USA NOAA/NCEP at 1/12° $\times$ 1/12° resolution (Gemmill et al., 2007) and are updated daily.
Model output: hourly (lowest 11 vertical levels) for D3, 3-hourly for D1 and D2. Time step in most simulations: approx. 106 seconds.
One-way nested domains; 5 grid point nudging zone.
Spectral nudging on D1 only and above level 10; wavenumber 9 and 6 in the zonal and meridional direction. Nudging coefficient 0.0003 s^{-1} for wind, temperature and specific humidity. No nudging in the PBL.
Physical parameterizations:
Precipitation: WRF Single-Moment 5-class scheme (option 4), Kain-Fritsch cumulus parameterization (option 1) turned off on D3.
Radiation: RRTM scheme for longwave (option 1); Dudhia scheme for shortwave (option 1)
PBL and land surface: Mellor-Yamada (MYJ) PBL scheme Mellor and Yamada (1982) (option 2), MM5 similarity (option 2) surface-layer scheme, and Noah Land Surface Model (option 2).
Surface roughnesses are kept constant at their winter (lower) value.
Diffusion: Simple diffusion (option 1); 2D deformation (option 4); 6th order positive definite numerical diffusion (option 2); rates of 0.06, 0.08, and 0.1 for D1, D2, and D3, respectively; vertical damping.
Positive definite advection of moisture and scalars.

Table 1: Summary of model and system setup and physical parameterizations used in the simulations.

The WRF model has been setup with the MODIS (2001-2010) land-cover classification of the International Geosphere-Biosphere Programme. The map of landcover classification for the inner domain is shown in Fig. 2. The most dominant class is Open Shrubland (Class 7) covering over 16% of the model grid; over 56% is covered by water.

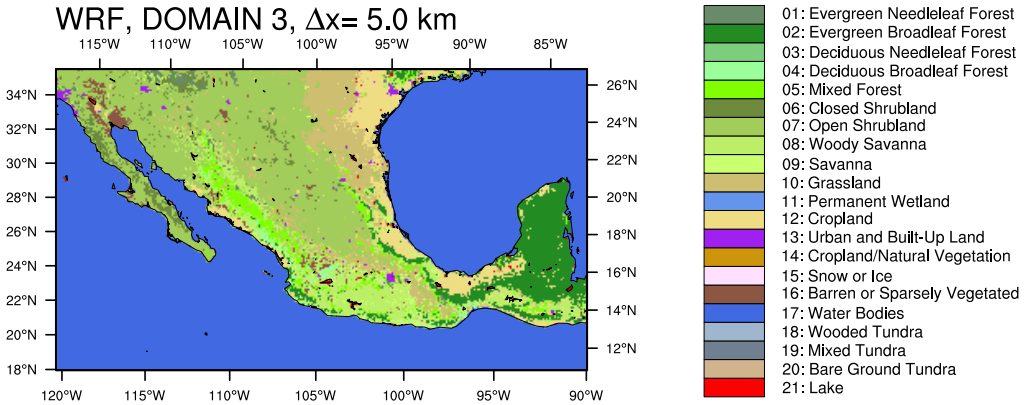

Figure 2: Land use categories for the WRF domain 3.

Most choices in the model setup are fairly standard and used by other modeling groups. The only special setting for wind energy applications is the use of a constant surface roughness length, thus disabling the annual cycle available in the WRF model. Surface roughnesses are kept constant at their winter value; a map for the innermost domain, D3, is given in Fig. 3. A table with the new surface roughness values is presented in Table 2. A large portion of the Mexican land area has an assigned 0.03 m roughness, coastal areas in the Gulf of Mexico have a surface roughness of 0.1 m and most of the Yucatan is covered by forest with a roughness of 0.9 m.

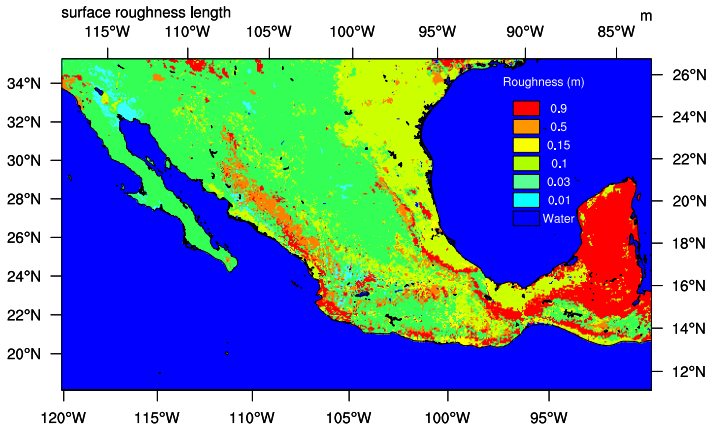

Figure 3: Surface roughness length (m) used in the WRF domain 3.

MODIS Landuse class	Min/Max stand roughness (m)	New roughness (m)
Evergreen Broadleaf Forest	0.50/0.50	0.90
Mixed Forests	0.20/0.50	0.50
Grasslands	0.10/0.12	0.10
Closed Shrublands	0.01/0.05	0.03
Croplands	0.05/0.15	0.10
Woody Savannas	0.01/0.05	0.03
Urban and Built-Up	0.50/0.50	0.50
Cropland/natural vegetation mosaic	0.05/0.14	0.10
Barren or Sparsely Vegetated	0.01/0.01	0.01

Table 2: Surface roughness length (m) as a function of landuse class for the standard WRF (minimum and maximum) and the modified values for the Mexico simulations.

3 The WRF Wind Atlas Method

The wind atlas method is based on the generalization of the wind climatologies derived from the mesoscale modeling. This generalization post-processing method has been used extensively in a number of wind resource assessment studies, particularly within the KAMM-WAsP method. The KAMM-WAsP method was adapted to use output from WRF simulations and it was first documented for the wind atlas of South Africa (Hahmann et al., 2014).

The post-processing allows a proper verification to be carried out, in which wind climate estimates derived from mesoscale modeling and measurements can be compared. Without the post-processing step no verification is possible, because the surface description within the model does not agree with reality, and therefore model winds will not agree with measured winds, except perhaps in extremely simple terrain or over water far from coasts. In addition to verification, the generalization method can be used to generate input files for WAsP that then are used to make microscale simulations and estimate the wind power resources at a local site.

3.1 Generalization factors

Four main parameters can be derived from the WRF model grid as described in Badger et al. (2014): (1) a factor that accounts for how the mesoscale model description of topography impacts the local flow, (2) a parameter that takes into account how the topography alters the mesoscale wind direction, (3) a parameter that accounts for the local flow perturbation on wind speed due to roughness length variations, and finally a (4) grid point dependent upstream roughness length. These four parameters are computed from the WRF grid description, that includes the topographic height and an average surface roughness length. These parameters are stored in a NetCDF file and used in the generalization of the WRF time series (see equations 1, 2 and 3).

3.2 Sectorization

To apply the generalization procedure to the WRF-model output, winds from the mesoscale model simulations are binned according to wind speed (in 1.0–2.5 $\mathrm{m\,s^{-1}}$ bins), wind direction (in 12–48 sectors) and seven stability classes based on the Obukhov length, which is also an output from the WRF simulation. The ranges for the stability classes are listed in Table 3 together with the "typical" length used in the generalization.

In practice, the whole WRF model grid of wind speed and directions for each model time step is binned according to the criteria above. These binned values are stored in a NetCDF file (see Section 4.2). The generalization procedure is then carried out on for each grid point and each desired level.

Stability class	Obukhov length range (m)	Typical Obukhov value $\tilde{L}$ (m)
Very unstable	$-50 \leq L < -100$	-75
Unstable	$-100 \leq L < -200$	-150
Near unstable	$-200 \leq L < -500$	-350
Neutral	$\|L\| < 500$	10000
Near stable	$200 \leq L < 500$	350
Stable	$50 \leq L < 200$	125
Very stable	$10 \leq L < 50$	30

Table 3: Stability ranges and typical values used in the generalization procedure.

3.3 Basic generalization equations

From the binning (section 3.2), mean values of wind speed, $\overline{u}$, and wind direction, $\overline{\phi}$ and typical Obukhov length $\tilde{L}$, together with their frequency of occurrence, F, of each bin are determined. For simplicity, we will drop the over-bar from the equations that follow, but it is understood that they are applied to the mean values of each bin and not the individual time series values. The central values wind speed and direction of each bin are corrected for changes in orography and roughness, which are a function of the sector and the height above ground. This correction gives us intermediate values, $\hat{u}$ and $\hat{\phi}$, which are given by

$$\hat{u} = \frac{u}{(1+\delta A_o)(1+\delta A_r)} \tag{1}$$

$$\hat{\phi} = \phi - \delta\phi_o, \tag{2}$$

where δA_o, $\delta\phi_o$ and δA_r and are generalization factors for orography in wind speed and direction and roughness change, respectively, described in section 3.1 above. From the corrected wind speed value we obtain an intermediary friction velocity, $\hat{u}_*$

$$\hat{u}_* = \frac{\kappa\hat{u}}{\ln[(z/\hat{z}_0) - \psi(z/\tilde{L})]} \tag{3}$$

where $\hat{z}_0$ is the downstream surface roughness length and ψ is a stability correction function that adjust the logarithmic wind profile due to non-neutral stability conditions and κ is the von Kármán constant. The stability correction uses the relationship:

$$\psi(z/L) = \begin{cases} -31.58[1-\exp(-0.19\,z/L)] & \text{if } z/L \geq 0 \\ 2\log[0.5(1+x)] + \log[0.5(1+x^2)] - 2\tan^{-1}(x) + 1.5746 & \text{if } z/L < 0 \end{cases} \tag{4}$$

where $x = (1-19z/L)^{1/4}$. We use this function with a typical value of the Obukhov length from each wind class bin (see Table 3), which avoids the use of the similarity theory on wind profiles that lie outside the bounds of validity of the theory and that sometimes occur in the WRF simulations. The use of the stability correction function is an option of the generalization method and it can be turned on or off (Method 3 is "on"; Method 4 is "off").

In the next step, we use the geostrophic drag law, which is used for neutral conditions to determine nominal geostrophic wind speeds, $\hat{G}$, and wind directions, α_G, are calculated, using the intermediate friction velocity and wind direction:

$$\hat{G} = \frac{\hat{u}_*}{\kappa}\sqrt{\left(\ln\frac{\hat{u}_*}{|f|\,\hat{z}_0} - A\right)^2 + B^2}, \tag{5}$$

$$\hat{\phi}_G = -\sin^{-1}\left(\frac{B\,\hat{u}_*}{\kappa\hat{G}}\right), \tag{6}$$

where $A = 1.8$ and $B = 5.4$ ($B = -5.4$ in the Southern Hemisphere) are two empirical parameters and f is the Coriolis parameter, and $\hat{\phi}_G$ is the angle between the near-surface winds and the geostrophic wind.

To obtain a new generalized friction velocity, $\hat{u}_{*G}$, for a standard roughness length $z_{0,std}$, Equation 5 is reversed by an iterative method, i.e.

$$\hat{G} = \frac{\hat{u}_{*G}}{\kappa}\sqrt{\left(\ln\frac{\hat{u}_{*G}}{f\,z_{0,std}} - A\right)^2 + B^2}, \tag{7}$$

Finally, the generalized wind speed, u_G, is obtained from $\hat{u}_{*G}$ by using the logarithmic wind profile law at the original height of the model output

$$u_G = \hat{u}_{*G}\,\kappa\ln(z/z_{0,std}). \tag{8}$$

3.4 Weibull distribution fit

The frequency distribution of the horizontal wind speed can often be reasonably well described by the Weibull distribution function (Tuller and Brett, 1984):

$$F(u) = \frac{k_w}{A_w}\left(\frac{u}{A_w}\right)^{k_w-1}\exp\left[-\left(\frac{u}{A_w}\right)^{k}\right], \tag{9}$$

where $F(u)$ is the frequency of occurrence of the wind speed u. In the Weibull distribution the scale parameter A_w has wind speed units and is proportional to the average wind speed calculated from the entire distribution. The shape parameter $k(\geq 1)$ describes the skewness of the distribution function. For typical wind speed distributions, the k_w-parameter has values in the range of 2 to 3.

From the values of A_w and k_w, the mean wind speed $\overline{U}$ ($\mathrm{m\,s^{-1}}$) and mean power density $\overline{E}$ ($\mathrm{W\,m^{-2}}$) in the wind can be calculated from:

$$\overline{U} = A_w\Gamma\left(1+\frac{1}{k_w}\right) \tag{10}$$

$$\overline{E} = \frac{1}{2}\rho A_w^3\cdot\Gamma\left(1+\frac{3}{k_w}\right) \tag{11}$$

where ρ is the mean density of the air and Γ is the gamma function. We use the moment fitting method as used in the Wind Atlas Analysis and Application Program (WAsP) for estimating the Weibull parameters. The method is described in detail in Troen and Petersen (1989). Basically this method estimates A_w and k_w to fit the power density in the time series instead of the mean wind speed.

The Weibull fit is done for the ensemble of wind speeds in each wind direction bin (usually 12 direction sectors) for each standard height (usually 5 heights: 10, 25, 50, 100 and 200 m) and standard roughness lengths (usually 5 roughness: 0.0002 (water), 0.03, 0.1, 0.4, 1.5 m). The 25 Weibull fits for each wind direction sector use the method described above.

This sector-wise transformation of Weibull wind statistics—i.e. transforming the Weibull A_w and k_w parameters to a number of reference heights over flat land having given reference roughnesses—uses not only the geostrophic drag law, but also a perturbation of the drag law, with the latter part including a climatological stability treatment. The transformation and stability calculation is consistent with that implemented in WAsP and outlined in Troen and Petersen (1989), with further details given in Kelly et al. (2014). The transformation is accomplished via perturbation of both the mean wind and expected long-term variance of wind speed, such that both Weibull-A_w and k_w are affected. When purely neutral conditions (zero stability effects) are presumed for the wind statistics to be transformed, there is still a perturbation introduced, associated with the generalized (reference) conditions in the wind atlas. This perturbation uses the default stability parameter values found in WAsP; it is negated upon subsequent application of the generalized wind from a given reference height and roughness to a site with identical height and

surface roughness, using WAsP with its default settings. The climatological stability treatment in the generalization depends on the unperturbed Weibull parameters and effective surface roughness (Troen and Petersen, 1989), as well as the mesoscale output heights and wind atlas reference heights (though the latter disappears upon application of wind atlas data via WAsP).

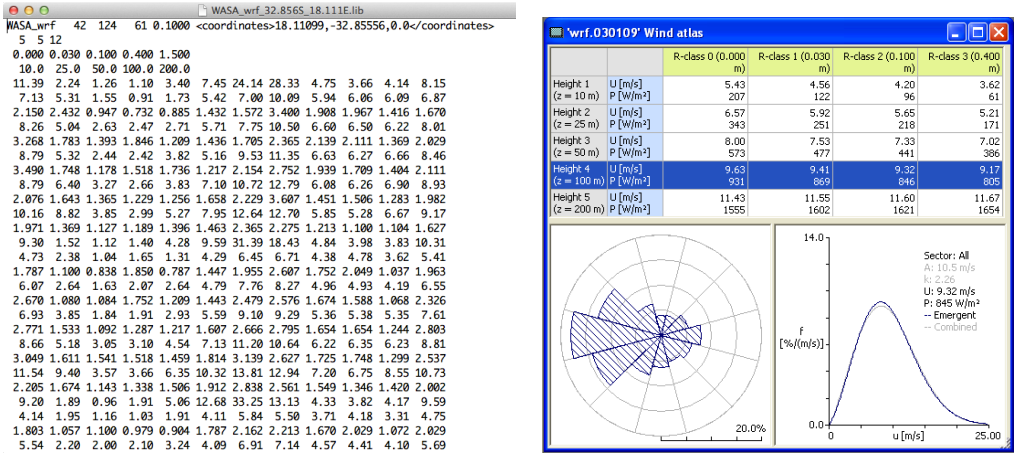

Figure 4: Format (left) and graphical view (right) of a WAsP "lib" file.

Figure 4 shows the structure of the resulting WAsP "lib" file. It is structured as Weibull A_wb's and k_w's for each sector, height and standard roughness length. The first row contains information about the geographical location of the wind climate represented in the lib-file. The second row lists the number of roughness classes (5), heights (5), and sectors (12), respectively. In the third and fourth row, the actual roughness (m) and heights (m) are listed. Below these header lines, a succession of frequencies of wind direction (1 line), values of Weibull-A_w (1 line) and Weibull-k_w (1 line) for each roughness class and height are printed for each sector (12 sectors per line). This type of file can be used and displayed (Figure 4) in WAsP.

4 Data processing

4.1 WRF files and data processing

The standard WRF code has been modified to output several variables relevant to wind energy applications. These key variables are: WSPD (wind speed from zonal and meridional wind components on their original staggered Arakawa-C grid interpolated to the coordinates of the mass grid), WDIR (wind direction from U and V, rotated and interpolated as for the wind speed), RHO (air density), ZNT (surface roughness length), RMOL (Inverse Obukhov length), USTAR (friction velocity) and variables necessary to obtain the height of the model levels. Other standard variables are added to aid in the interpretation of the results, e.g. temperatures, precipitation, etc.

As previously discussed, the 11-year WRF simulation was run in a series of 11-day long overlapping integrations, with the output from the first day being discarded. As each of these 10 days simulations is complete, the model output is concatenated into single "daily" files for a reduced number of vertical levels (12 half levels for Mexico). The key variables from the output from these daily files are further interpolated to five constant heights (namely 25, 50, 80, 100, and 150 meters) above the WRF model terrain. These we refer to as "wind" files (Table 4).

4.2 Generalization procedure

To generalize de WRF derived wind climatologies an additional step is taken. A fortran code has been developed to create a giant "TAB" file. In this file the number of samples is counted as a

```
netcdf winds_d03_2015-12-31 {
dimensions:
    south_north = 390 ;
    west_east = 687 ;
    lev = 5 ;
    DateStrLen = 19 ;
    Time = UNLIMITED ; // (23 currently)
variables:
    float LEVS(lev) ;
        LEVS:long_name = "heights AGL" ;
        LEVS:units = "meters" ;
    float WSPD(Time, lev, south_north, west_east) ;
        WSPD:long_name = "Wind speed" ;
        WSPD:units = "m/s" ;
    float WDIR(Time, lev, south_north, west_east) ;
        WDIR:long_name = "Wind direction" ;
        WDIR:units = "degrees" ;
    float RHO(Time, lev, south_north, west_east) ;
        RHO:long_name = "Density" ;
        RHO:units = "kg m-3" ;
    float UST(Time, south_north, west_east) ;
        UST:long_name = "u* in similarity theory" ;
        UST:units = "m/s" ;
    float RMOL(Time, south_north, west_east) ;
        RMOL:long_name = "1./Monin Ob. Length" ;
        RMOL:units = "1/m" ;
    char TIMES(Time, DateStrLen) ;
        TIMES:long_name = "UTC time" ;
data:

 LEVS = 25, 50, 80, 100, 150 ;
}
```

Table 4: Contents of a NetCDF "wind" file.

function of sector, stability (Table 3) and wind speed. Table 5 shows the structure of this file. The variable "FREQ" is a short and has dimensions of stability, wind speed bin, sector, and the geographical location, south_north, west_east. Because of the large size of the Mexico WRF domain, this file has been divided into two regions: West and East, reflected by the "corners" parameters in the file. The file also contains the mean wind speed (WSPD), mean density (RHOMEAN) and maximum wind speed (WMAX) of the period considered.

```
netcdf TabFile_East_d03_100m
dimensions:
    south_north = 390 ;
    west_east = 344 ;
    sector = 48 ;
    wind = 40 ;
    stab = 7 ;
    level = 1 ;
variables:
    float XLAT(south_north, west_east) ;
        XLAT:long_name = "latitude" ;
        XLAT:units = "degree_north" ;
    float XLON(south_north, west_east) ;
        XLON:long_name = "longitude" ;
        XLON:units = "degree_east" ;
    float ALPHA(south_north, west_east) ;
        ALPHA:long_name = "grid rotation angle" ;
        ALPHA:units = "degrees" ;
    float RHOMEAN(south_north, west_east) ;
        RHOMEAN:long_name = "Density" ;
        RHOMEAN:units = "kg/m3" ;
    float LEV(level) ;
        LEV:long_name = "Level height" ;
        LEV:units = "m/s" ;
    float WSPD(south_north, west_east) ;
        WSPD:long_name = "Averaged wind" ;
        WSPD:units = "m/s" ;
    float WMAX(south_north, west_east) ;
        WMAX:long_name = "Maximum wind speed" ;
        WMAX:units = "m/s" ;
    short FREQ(stab, wind, sector, south_north, west_east) ;
        FREQ:long_name = "Wind frequency" ;
        FREQ:units = "frequency" ;
        FREQ:scale_factor = 1.f ;
        FREQ:add_offset = 0.f ;
    float Ltypical(stab) ;
        Ltypical:long_name = "L typical" ;
        Ltypical:units = "m" ;
    float wspdCl(wind) ;
        wspdCl:long_name = "Velocity of bin centre" ;
        wspdCl:units = "m/s" ;
    float wdirCl(sector) ;
        wdirCl:long_name = "Wdir of each bin" ;
        wdirCl:units = "Degree" ;

// global attributes:
        :start_date = "2005-10-01" ;
        :end_date = "2015-09-30" ;
        :maxWind = 40.f ;
        :corners = 344, 687, 1, 390 ;
```

Table 5: Contents of a NetCDF “TAB” file.

5 Preliminary verification

5.1 General assessment

Here we perform a preliminary verification of the WRF Pre-run numerical wind atlas (NWA) results against measurements. These measurements have been processed and analyzed in the report "D2.1 and D2.3: Analysis of historic data". We compare the mean generalized wind speed at 50 m and standard surface roughness length of 0.03 m (Fig. 6). Only stations with anemometer heights above 40 m have considered in the analysis (see their location in Fig 5). Also, only full years of data were considered in both the observed and WRF Pre-run estimates. The generalization of the tall mast observations was carried out by using WAsP with SRTM terrain elevation for an area of 40 km $\times$ 40 km around each site. Since the roughness of the area around a site was not readily available, the WAsP default value of 3cm is used for the roughness parameter.

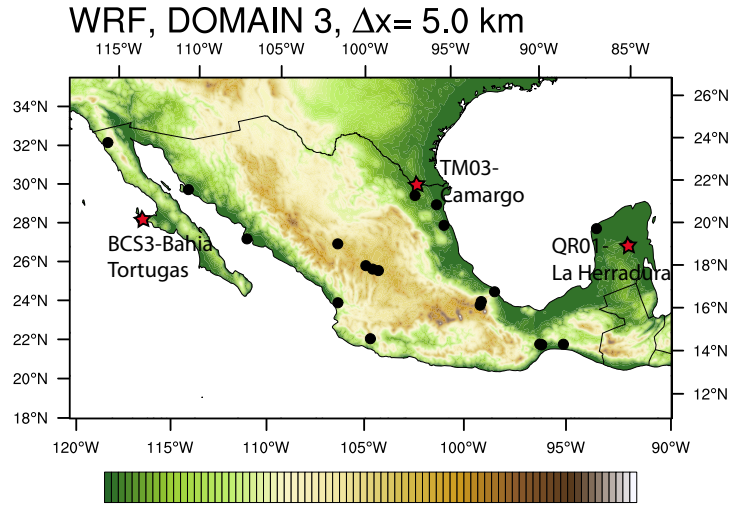

Figure 5: Location of the 23 tall masts used in the preliminary validation of the WRF Pre-run. The three sites used for more detailed inspection are shown by a red star.

The preliminary validation shows considerable differences between observed and simulated NWA. However, two major issues are relevant here. Firstly, 15 of the 23 stations are located in sites with low wind resources (i.e. generalized winds with speeds below 6 m s^{-1}). The winds at these sites are often a challenge for numerical weather prediction models to simulate. However, all the sites identified as low winds in the observations are also predicted as low in the WRF Pre-run. Secondly, the four sites where the WRF Pre-run severely over predicts the wind resources are concentrated in the high resource area of the well known region of the Istmo of Tehuantepec in the states of Oaxaca and Chiapas. Three of the four stations are within 12 km of each other. The reason for the high winds in the WRF Pre-run are unknown and will be investigated in future work of the project.

5.2 Specific examples

We show examples of verification for three stations: BCS3 - Bahía Tortugas (Baja California Sur), QR01 - La Herradura (Quintana Roo, Yucatan Peninsula) and TM03 - Camargo (Tamaulipas).

5.2.1 BCS3 - Bahía Tortugas

The mast Bahía Tortugas (Fig. 7) is located along the west coast of Baja California Sur. Generalized winds are weak (4.89 m s^{-1} in the observations, 4.82 m s^{-1} in the WRF Pre-run). From

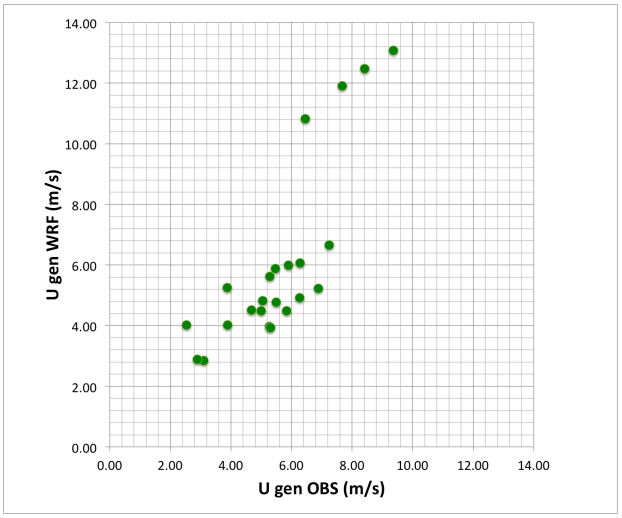

Figure 6: Comparison of annual mean generalized wind speed ($\mathrm{m\,s^{-1}}$) simulated by WAsP (using a uniform roughness of 3 cm around each site) and WRF Pre-run for the 23 stations described in the analysis of historical data report. The station locations are in Fig. 5. The winds are generalized for 50 m height AGL and a standard surface roughness length of 0.03 m.

the observations, winds are from SW to NE, with a more pronounce sector from the West. In the WRF Pre-run, winds are mostly from the NWW, probably a signature of sea breeze.

5.2.2 QR01 - La Herradura

The mast La Herradura (Fig. 8) is located deep within the Yucatán Peninsula over a region dominated by tropical forest. The generalized wind roses from the observations and the WRF Pre-run are quite similar, with a dominant sector from the SE. However, the WRF Pre-run overestimates the annual mean wind. This is probably a result of the surface roughness used in the WAsP calculation (uniform 3 cm) which is not appropriate for forested landscapes and makes the generalized winds too low.

5.2.3 TM03 - Camargo

The mast Camargo (Fig. 9) is located in NE Mexico along the border with the USA. Here the generalized wind roses are dominated by winds from the S–SE. The rose from the WRF Pre-run is slightly counterclockwise rotated when compared to the observations. Annual mean winds and distributions compare well between the model and the observations.

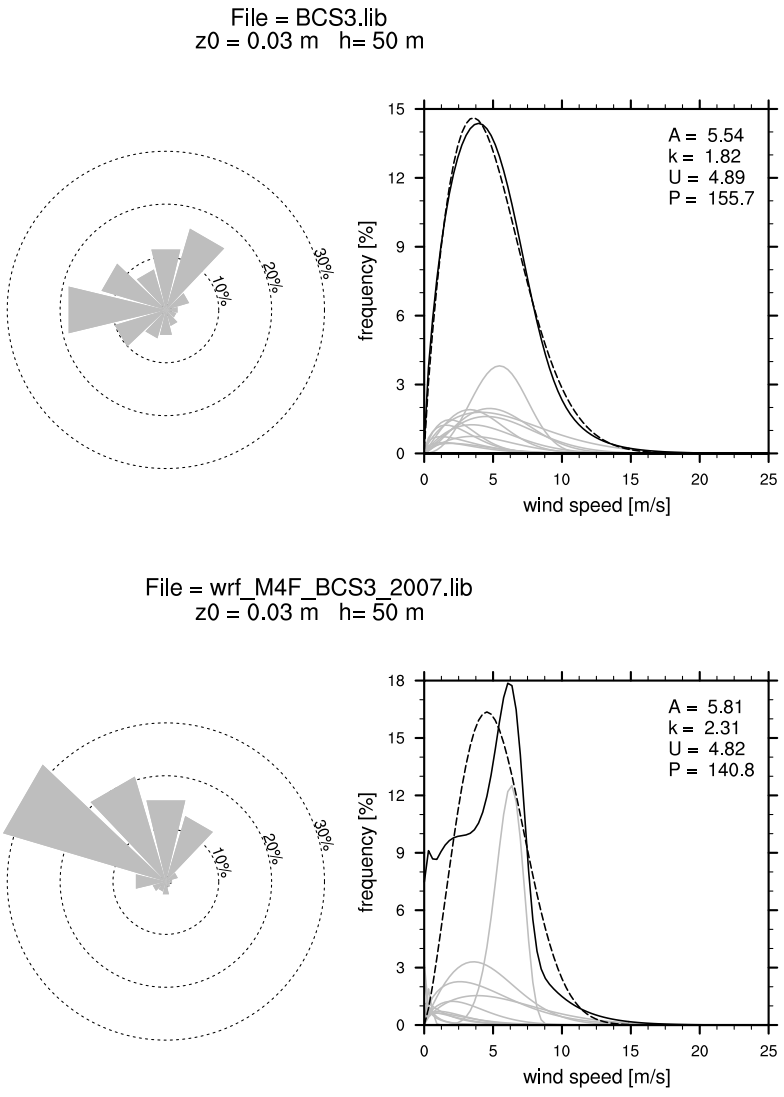

Figure 7: Generalized wind rose and wind distributions for 50 m and surface roughness of 0.03 m at BCS3 - Bahía Tortugas for 2007: simulated by WAsP from observations (top); simulated by WRF Pre-run (bottom).

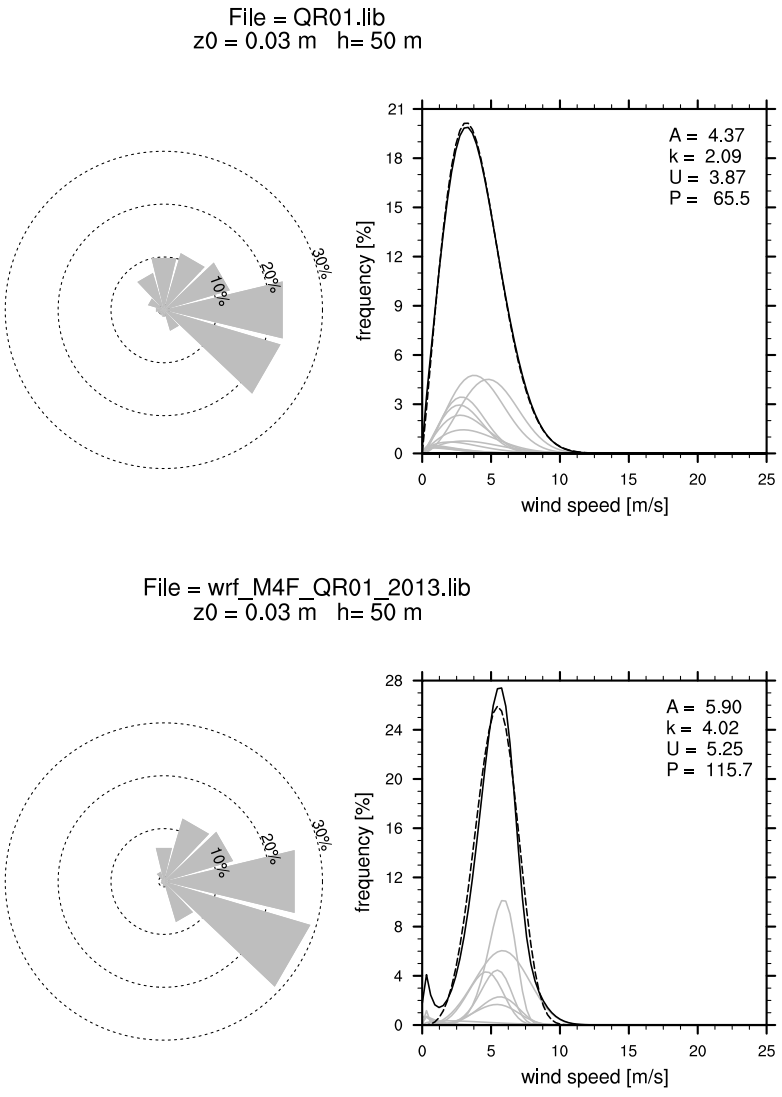

Figure 8: Generalized wind rose for 50 m and surface roughness of 0.03 m at QR01 - La Herradura for 2013: simulated by WAsP from observations (top); simulated by WRF Pre-run (bottom).

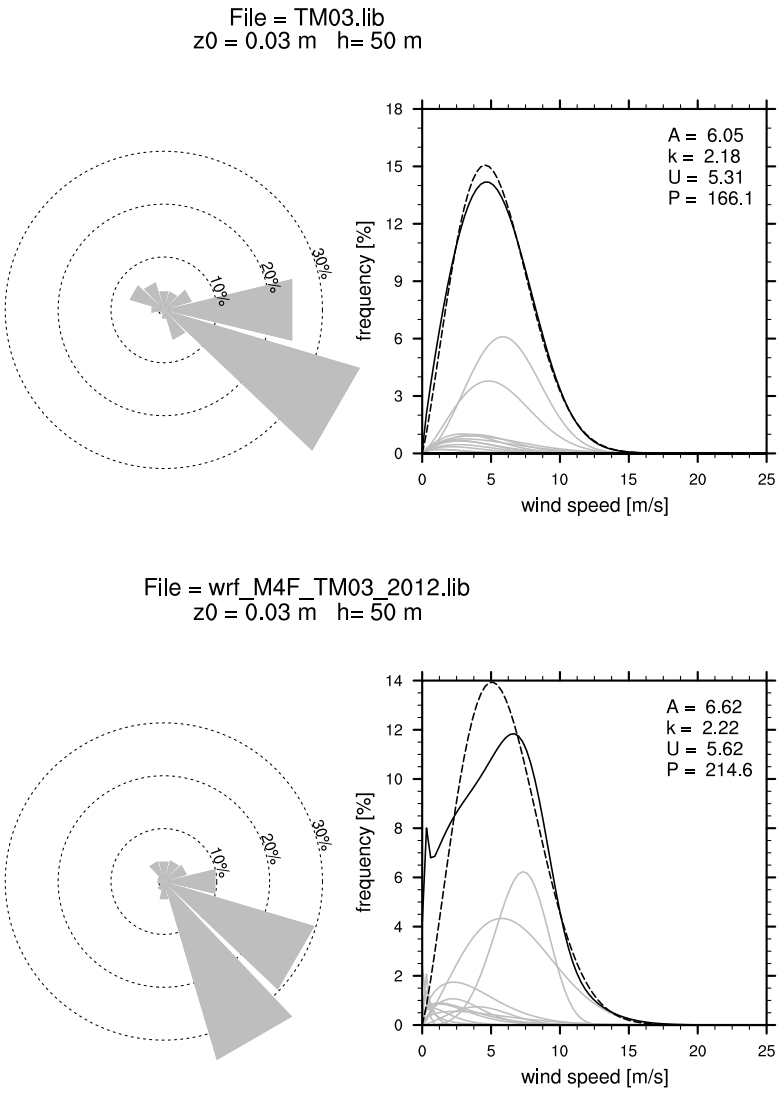

Figure 9: Generalized wind rose for 50 m and surface roughness of 0.03 m at TM03 - Camargo for 2012: simulated by WAsP from observations (top); simulated by WRF Pre-run (bottom).

6 Wind atlas maps

6.1 Mean annual maps

Maps of the WRF-based numerical wind atlas are now presented. The averages correspond to the period of simulation 1 October 2005 – 30 September 2015.

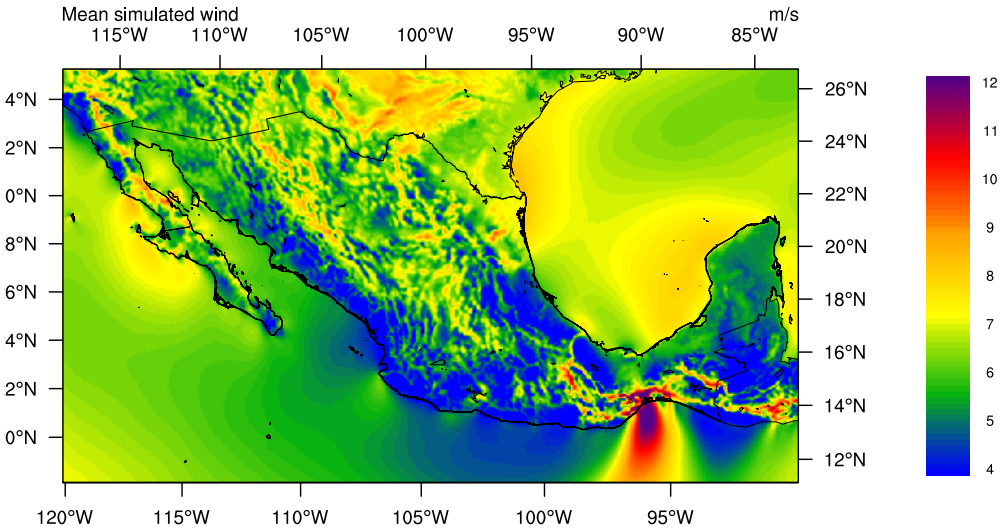

Figure 10: Annual mean simulated wind speed at 100 m AGL from the WRF-based numerical wind atlas. The color scale to the right hand side is in m s^{-1}.

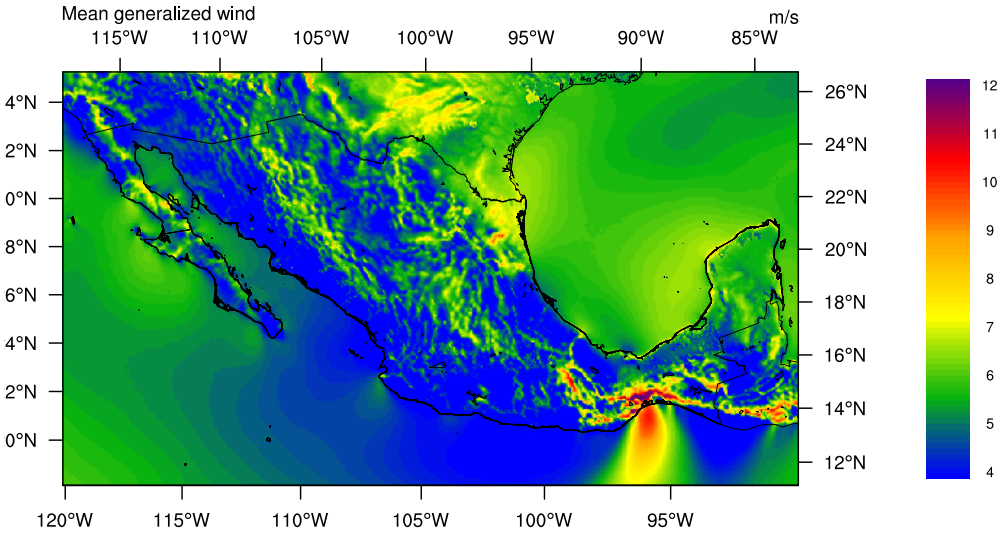

Figure 11: Annual mean generalized wind speed (to $z_0 = 0.1$ m) at 100 m AGL from the WRF-based numerical wind atlas. The color scale to the right hand side is in m s^{-1}.

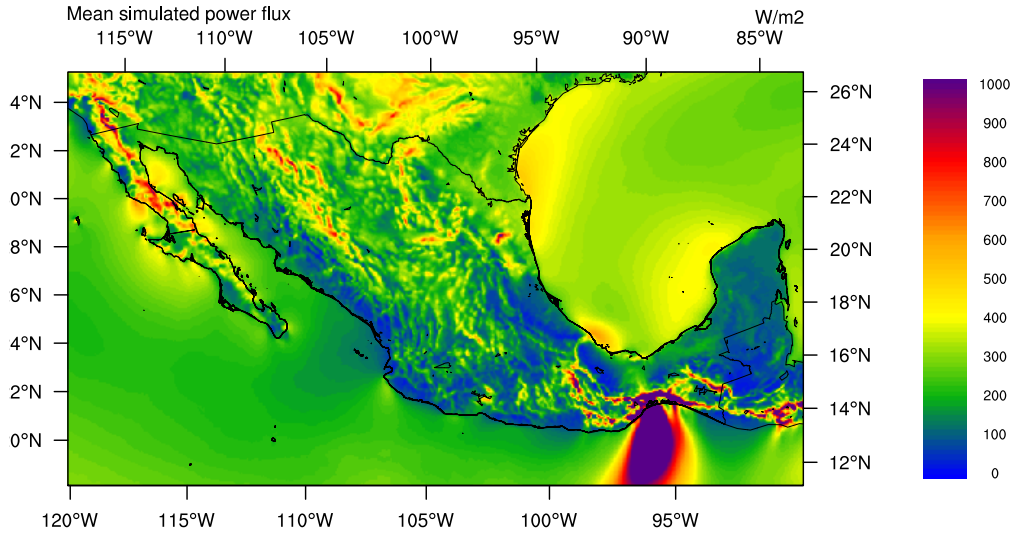

Figure 12: Annual mean simulated wind power density at 100 m AGL from the WRF-based numerical wind atlas. The color scale to the right hand side is in W m^{-2}.

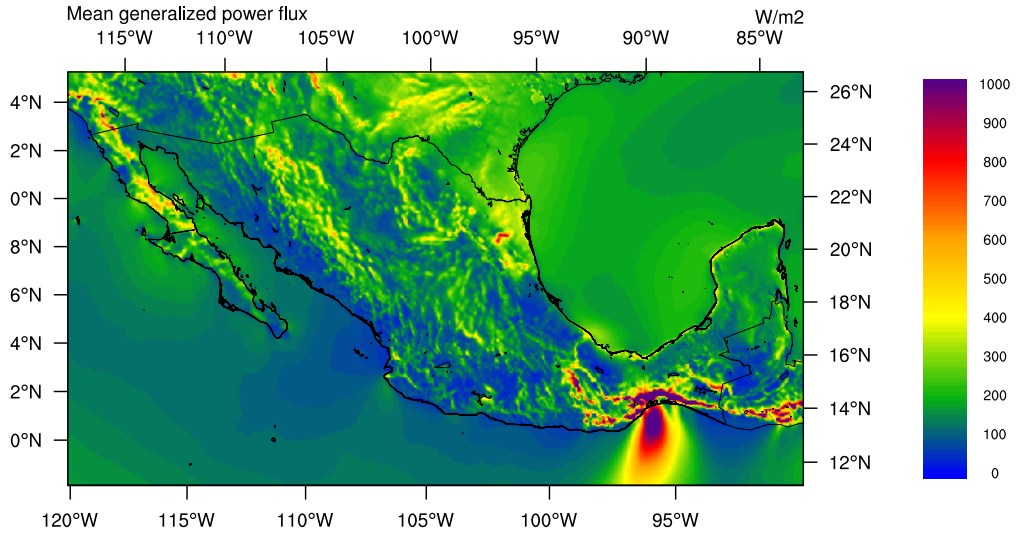

Figure 13: Annual mean generalized wind power density (to $z_0 = 0.1$ m) at 100 m AGL from the WRF Pre-run numerical wind atlas. The color scale to the right hand side is in W m^{-2}.

6.2 Variability maps

6.2.1 The annual cycle of wind speed

Figure 14 shows the 2006–2015 mean in simulated wind speed at 100 m. Mean wind speeds in the Itsmo show a strong annual cycle with stronger winds from November to March. Other regions with strong a annual cycle are along the Gulf of California and the northern part of the Gulf og Mexico.

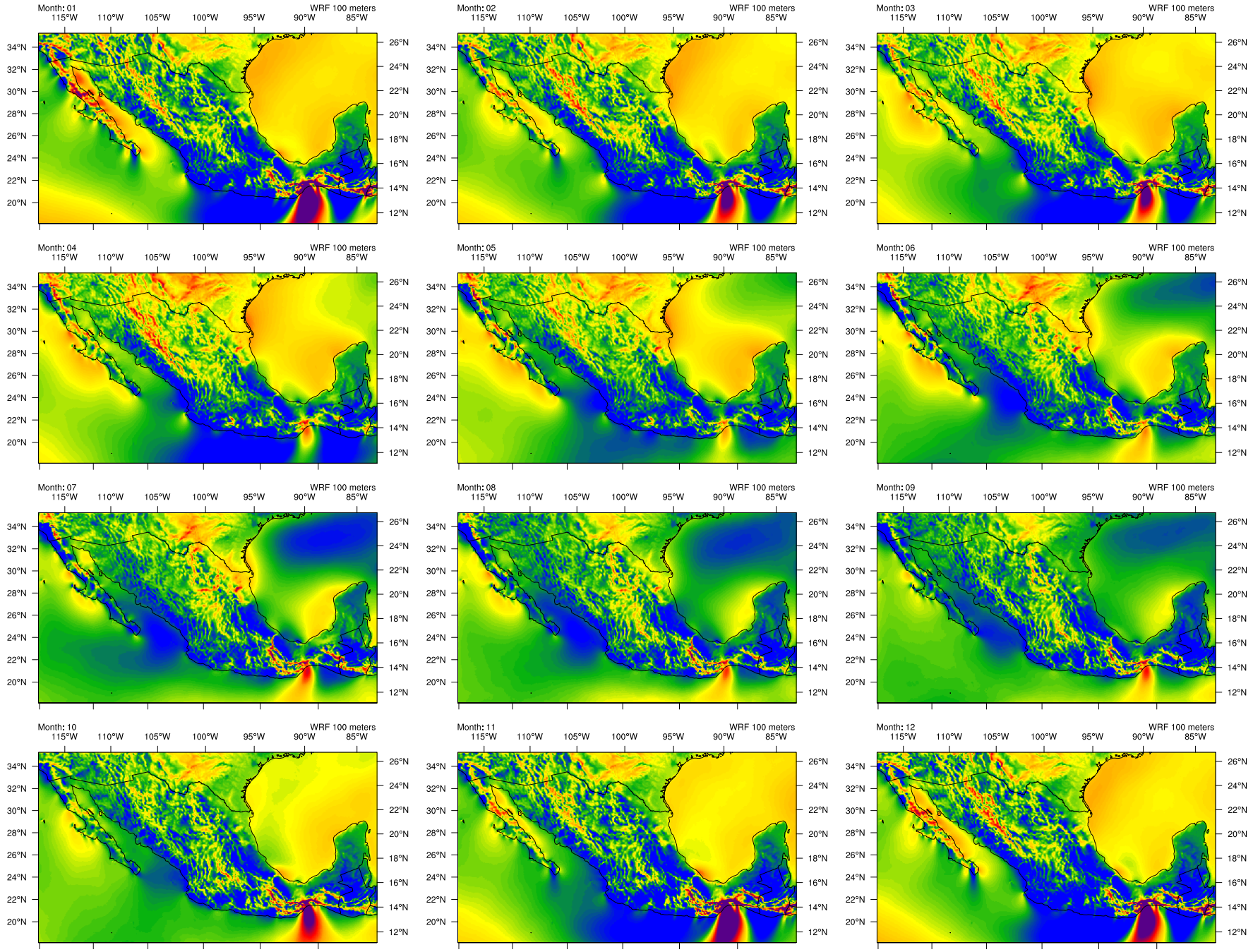

Figure 14: Monthly mean (2006–2015) simulated wind speed ($m\,s^{-1}$) at 100 m. Label as in Fig. 10.

6.2.2 Interannual variability of wind speed

Figure 15 shows the standard deviation of the annual mean (2006–2015) simulated wind speed at 100 m. The largest values ($\sim$0.5 m s^{-1} or $>$ 8%) are located offshore. Other significant areas are located along the coast in Veracruz and the southern tip of Baja California. The pattern of standard deviation along the Pacific coast off the Itsmo de Tehuantepec suggests that there might be slight changes in the location of the strongest winds from one year to the next in this region. The southern part is the most variable from year to year.

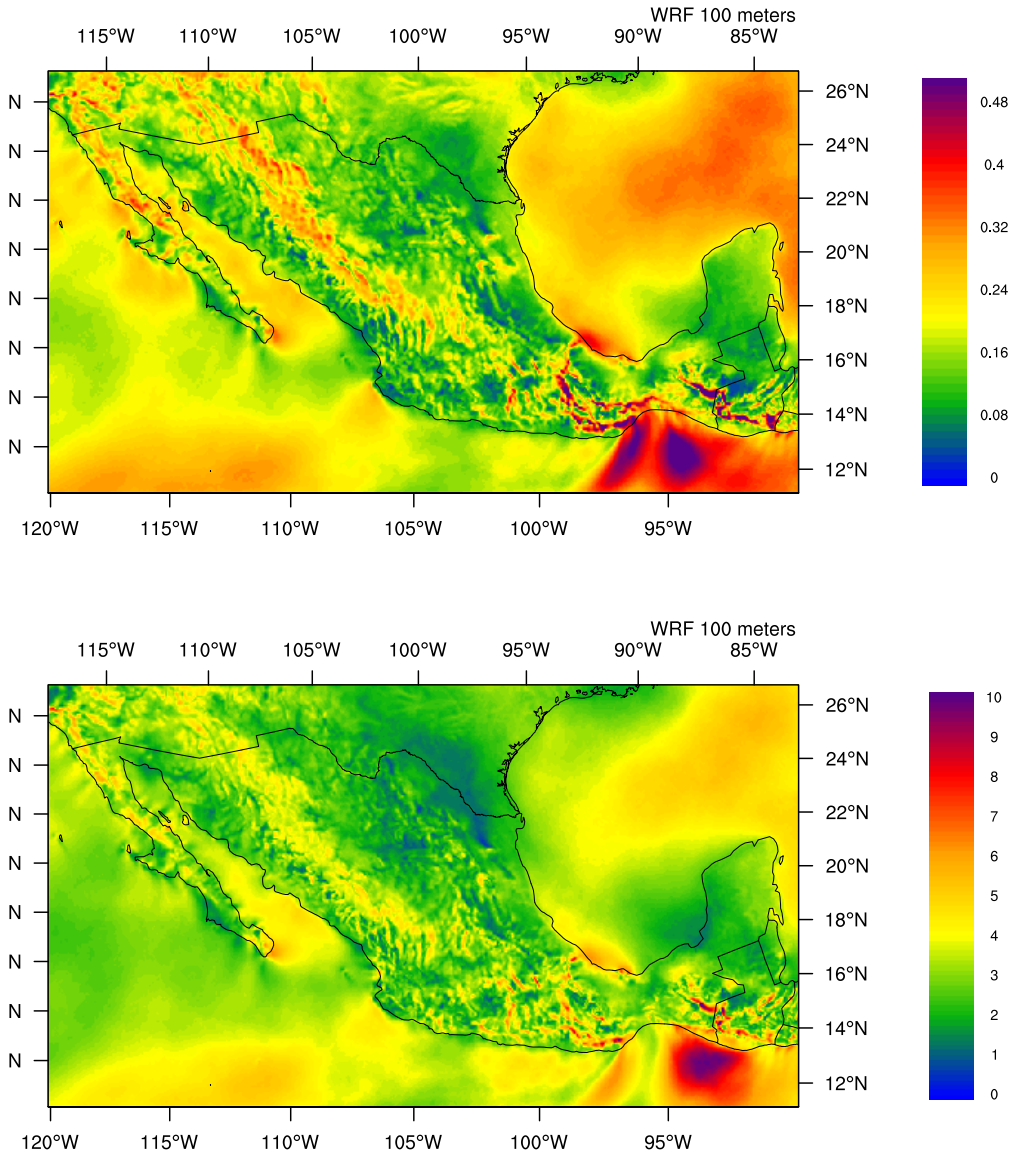

Figure 15: Standard deviation (σ, top, m s^{-1}) and relative standard deviation ($\sigma/\overline{U}$, bottom, %) of the annual mean simulated wind speed (2006–2015).

7 Summary and recommendations

Based on the results of the WRF Pre-run and its preliminary validation, we make the following recommendations to the sensitivity studies:

- The use of accurate surface roughness is important in both the WAsP calculations and in the WRF simulations. For the WRF simulations, an investigation of seasonal cycle of vegetation and its impact on the surface roughness should be carried out.
- The wind speed is severely over predicted in the region of the Istmo of Tehuantepec. Further investigation of the causes of this is important for the final wind atlas. Possible processes responsible for the inaccurate simulations are: (i) smooth topography, (ii) inaccurate surface roughness specification, (iii) lack of horizontal resolution resulting in (i) and/or (ii).

References

Badger, J., H. Frank, A. N. Hahmann, and G. Giebel, 2014: Wind-Climate Estimation Based on Mesoscale and Microscale Modeling: Statistical-Dynamical Downscaling for Wind Energy Applications. *J. Appl. Meteorol. Climatol.*, **53**, 1901–1919.
URL http://journals.ametsoc.org/doi/abs/10.1175/JAMC-D-13-0147.1

Dee, D. P., S. M. Uppala, A. J. Simmons, P. Berrisford, P. Poli, S. Kobayashi, U. Andrae, M. A. Balmaseda, et al., 2011: The ERA-Interim reanalysis: configuration and performance of the data assimilation system. *Q. J. R. Meteorolog. Soc.*, **137**, 553–597.

Gemmill, W., B. Katz, and X. Li, 2007: Daily real-time global sea surface temperature - high resolution analysis at NOAA/NCEP. Office note nr. 260, 39 pp, NOAA/NWS/NCEP/MMAB.

Hahmann, A. N., J. Badger, C. L. Vincent, M. C. Kelly, P. J. H. Volker, and J. Refslund, 2014: Mesoscale modeling for the wind atlas for South Africa (WASA) Project. Tech. rep., DTU Wind Energy.
URL http://orbit.dtu.dk/services/downloadRegister/107110172/DTU_Wind_Energy_E_0050.pdf

Hahmann, A. N., D. Rostkier-Edelstein, T. T. Warner, F. Vandenberghe, Y. Liu, R. Babarsky, and S. P. Swerdlin, 2010: A Reanalysis System for the Generation of Mesoscale Climatographies. *J. Appl. Meteor. Clim.*, **49**, 954–972.
URL http://dx.doi.org/10.1175/2009JAMC2351.1

Hahmann, A. N., C. L. Vincent, A. Peña, J. Lange, and C. B. Hasager, 2015: Wind climate estimation using WRF model output: Method and model sensitivities over the sea. *Int. J. Climatol.*, **35**, 3422–3439.
URL http://dx.doi.org/10.1002/joc.4217

Kelly, M. C., I. Troen, and H. E. Jørgensen, 2014: Weibull-k Revisited: "Tall" Profiles and Height Variation of Wind Statistics. *Boundary-Layer Meteorol.*, **152**, 107–124.

Mellor, G. L. and T. Yamada, 1982: Development of a turbulence closure model for geophysical fluid problems. *Rev. Geophys. and Space Phys.*, **20**, 851–875.

Troen, I. and E. L. Petersen, 1989: *European Wind Atlas*. Published for the Commission of the European Communities, Directorate-General for Science, Research, and Development, Brussels, Belgium by Risø National Laboratory.

Tuller, S. E. and A. C. Brett, 1984: The characteristics of wind velocity that favor the fitting of a Weibull distribution in wind-speed analysis. *J. Appl. Meteor. Clim.*, **23**, 124–134.

DTU Wind Energy is a department of the Technical University of Denmark with a unique integration of research, education, innovation and public/private sector consulting in the field of wind energy. Our activities develop new opportunities and technology for the global and Danish exploitation of wind energy. Research focuses on key technical-scientific fields, which are central for the development, innovation and use of wind energy and provides the basis for advanced education at the education.

We have more than 240 staff members of which approximately 60 are PhD students. Research is conducted within nine research programmes organized into three main topics: Wind energy systems, Wind turbine technology and Basics for wind energy.

Technical University of Denmark
Department of Wind Energy
Frederiksborgvej 399
Building 118
4000 Roskilde
Denmark
Telephone 46 77 50 85

info@vindenergi.dtu.dk
www.vindenergi.dtu.dk